A ketone functionlized luminescent terbium metal-organic framework for sensing of small molecules

Zhiyong Guo, [a] **Xuezhi Song,** [b] **Huaping Lei,** [c] **Hailong Wang,** [a] **Shengqun Su,** [b] **Hui Xu,** [d] **Guodong Qian,** [d] **Hongjie Zhang,*** [b] **Banglin Chen,*** [a]

[a] Department of Chemistry, University of Texas at San Antonio, San Antonio, TX 78249-0698, USA. E-mail: banglin.chen@utsa.edu

[b] State Key Laboratory of Rare Earth Resource Utilization, Changchun Institute of Applied Chemistry, Chinese Academy of Sciences, Changchun 130022 (China). E-mail: hongjie@ciac.ac.cn.

[c] Key Laboratory of Materials Physics, Institute of Solid State Physics, Chinese Academy of Sciences, Hefei 230031(China)

[d] State Key Laboratory of Silicon Materials, Department of Materials Science & Engineering, Zhejiang University, Hangzhou 310027 (China)

Experimental Section

Materials and Measurements. All reagents and solvents were used as received from commercial suppliers without further purification. H_3BCB was prepared according to the reported literature. ^1H NMR was obtained using a Varian INOVA 400 MHz spectrometer at room temperature. The elemental analyses were performed with PerkinElmer 240 CHN analyzers from Galbraith Laboratories, Knoxville, TN. Powder X-ray diffraction (PXRD) data were recorded on a Bruker D8 ADVANCE X-ray powder diffractometer using CuKα radiation (λ = 1.5405 Å). FTIR spectra were recorded within the 4000-400 cm^{-1} wavenumber range using a Bruker TENSOR 27 Fourier Transform Infrared Spectrometer (FT-IR) with the KBr pellet technique and operating in the transmittance mode. The luminescence decay curve was obtained from a Lecroy Wave Runner 6100 Digital Oscilloscope (1 GHz) using a tunable laser (pulse width = 4 ns, gate = 50 ns) as the excitation source (Continum Sunlite OPO). UV/Vis spectra were recorded on a Shimadzu UV-3600 spectrophotometer. N_2, H_2, C_2H_2, CH_4 and CO_2 adsorption isotherms were measured on ASAP 2020. A Coulter Omnisorp 100cx analyzer was used to measure methanol, ethanol, propanol, isopropanol sorption isotherm for activated **1a** formed by heating of the methanol exchanged **1** at the temperature of 200 ℃ under high vacuum overnight.

Fluorescence Measurements. The fluorescence properties of **1** and solvent included **1a** were investigated in the solid state at room temperature. A fresh sample (10 mg) of **1** was activated and then immersed into methanol solvent (10 mL) with different organic solvent (0.1 mL) to form solvent included **1a** which was collected by filtration and drying for 24 hours at 20 ℃. The sample was pressed on a glass slide for the photoluminescence studies. The fluorescence excitation and emission spectra were recorded at room temperature with a Hitachi F-4500 spectrophotometer equipped with a 150 W Xenon lamp as an excitation source. The photomultiplier tube (PMT) voltage was 700 V, the scan speed was 1200 nm/min. The slit widths of excitation and emission were set the same in each sensing experiment.

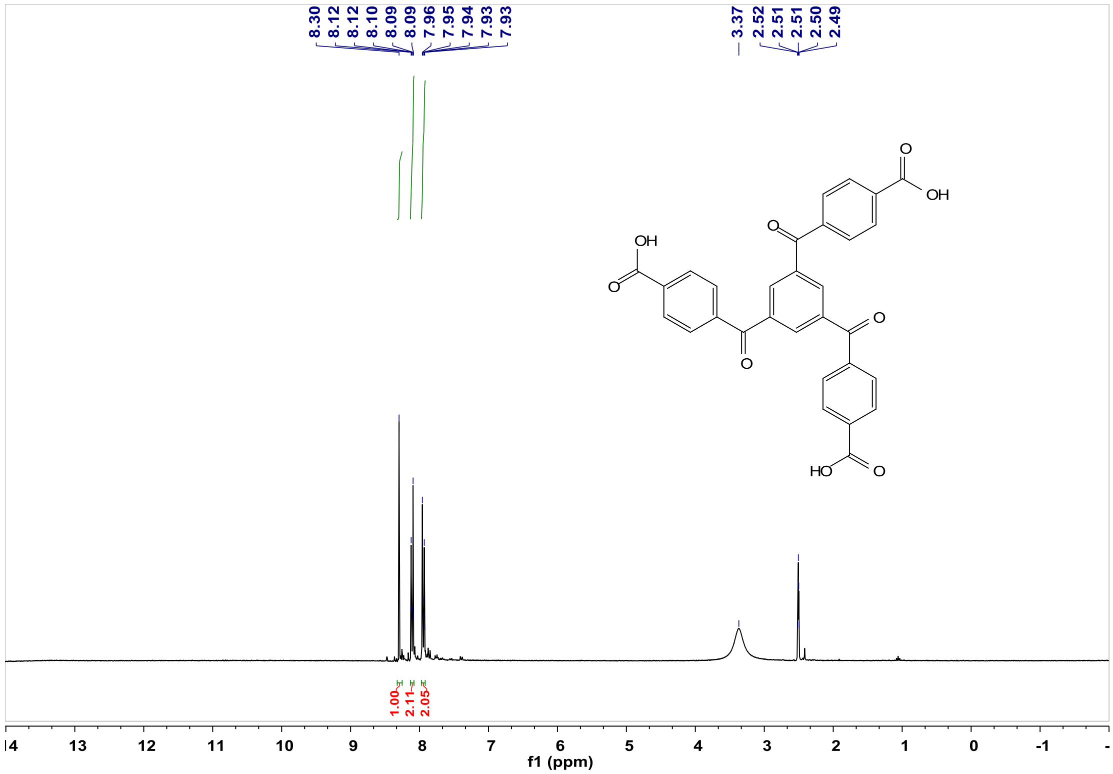

Figure S1. ^{1}H (DMSO-d6, 400MHz) spectra of the ligand H_3BCB.

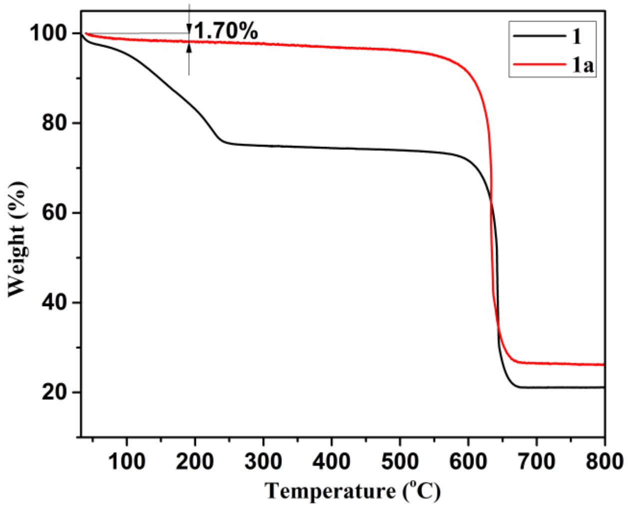

Figure S2. TGA traces of **1** and **1a** ranging from room temperature to 800 ℃ under N_2 atmosphere. From Room temperature to 200 ℃, the weight loss for **1a** is merely 1.70%. This indicates that most of solvent molecules in **1a** are removed after activated.

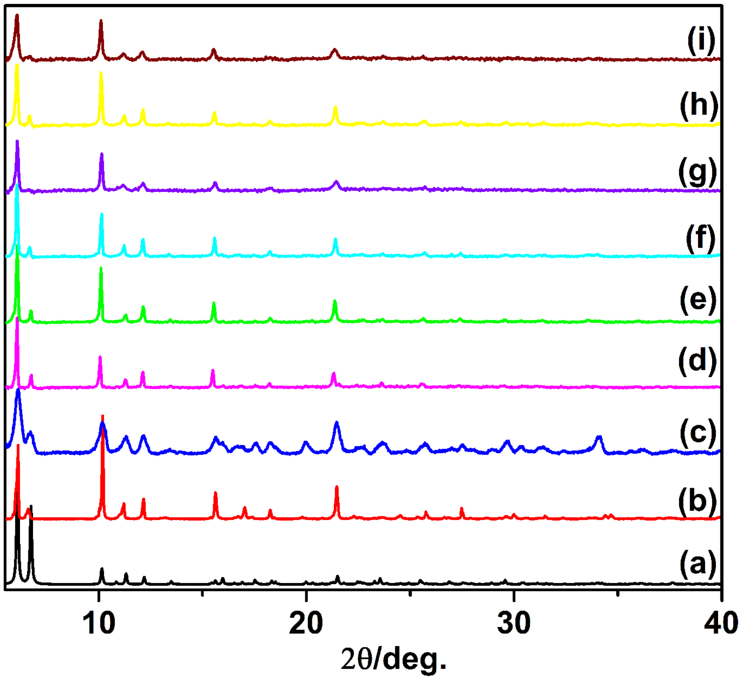

Figure S3. Powder XRD patterns of **1** (a) simulated, (b) as synthesized, (c) after gas sorption, (d) in methanol, (e) in nitrobenzene, (f) with phenol, (g) in benzaldehyde, (h) in benzonitrile, (i) in aniline.

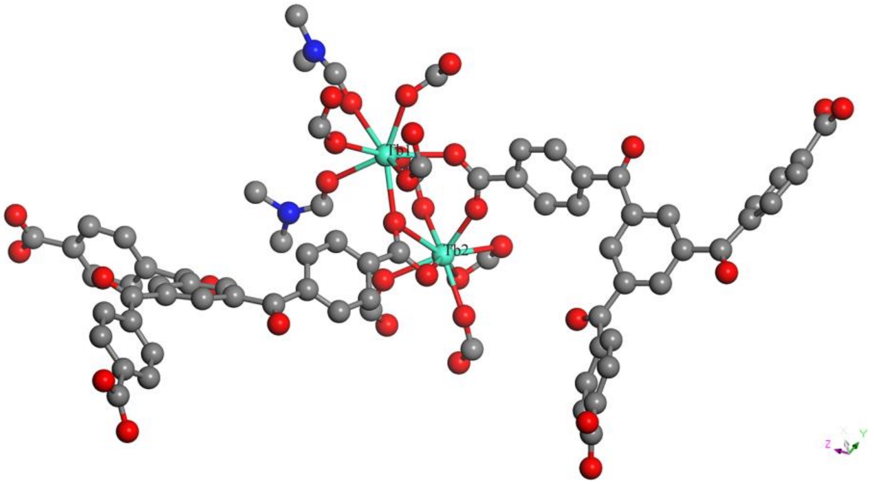

Figure S4. Ball-and-stick representation of the asymmetric unit in the crystal structure of **1**, hydrogen atoms and lattice solvent molecules are omitted for clarity (Tb, cyan; O, red; N, blue; C, grey).

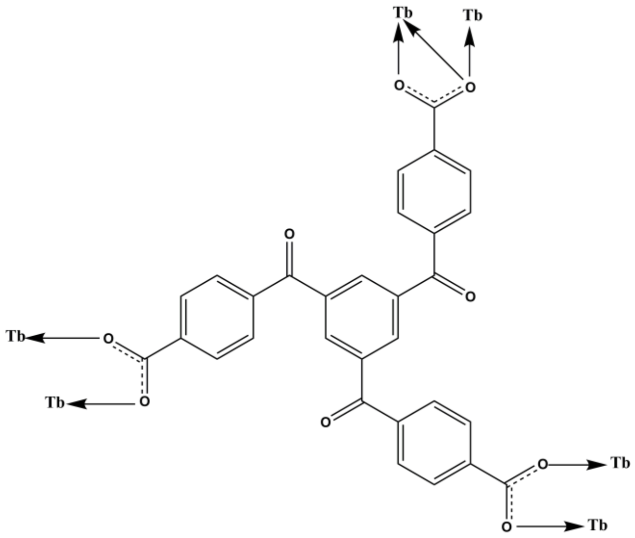

Figure S5. Coordination mode of ligand H_3BCB in **1**.

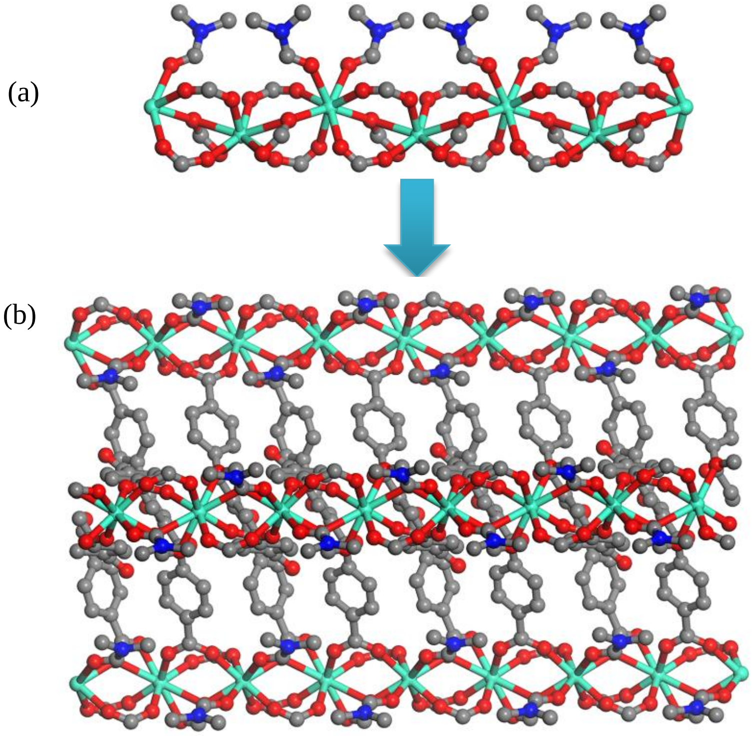

Figure S6. (a) Each one-dimensional inorganic chain along the [001] direction with a threefold screw axis (b) connected to each other lead to impenetrable organic walls along [100] direction (Tb, cyan; O, red; N, blue; C, grey). H atoms are omitted for clarity.

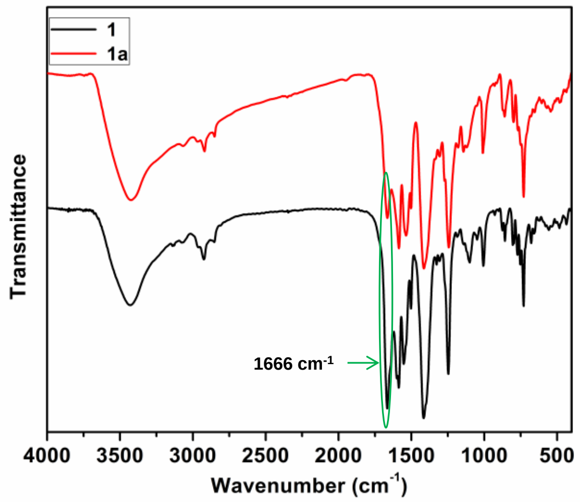

Figure S7. FTIR of **1** (black) and **1a** (red).

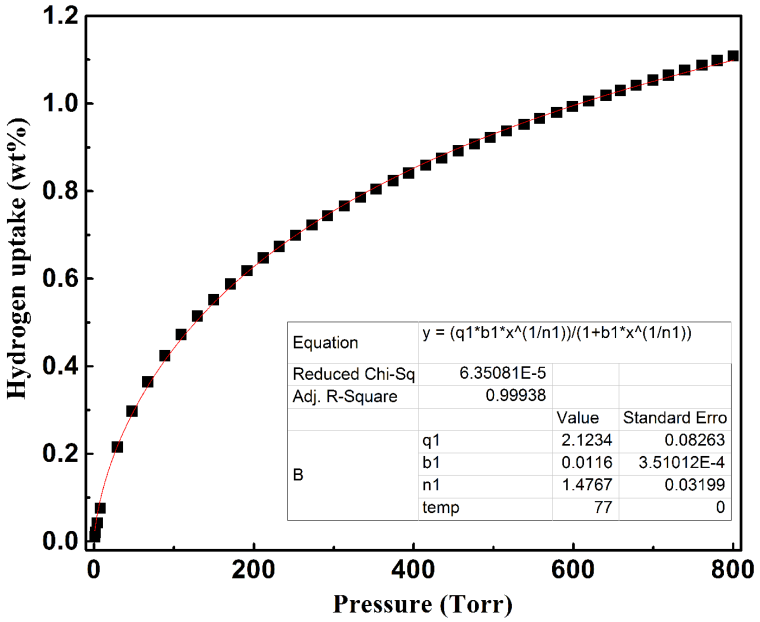

Figure S8. Gas sorption isotherm of **1a** for H_2 at 77 K. The red curve represents the fitting H_2 sorption data using Langmuir-Freundlium equation.

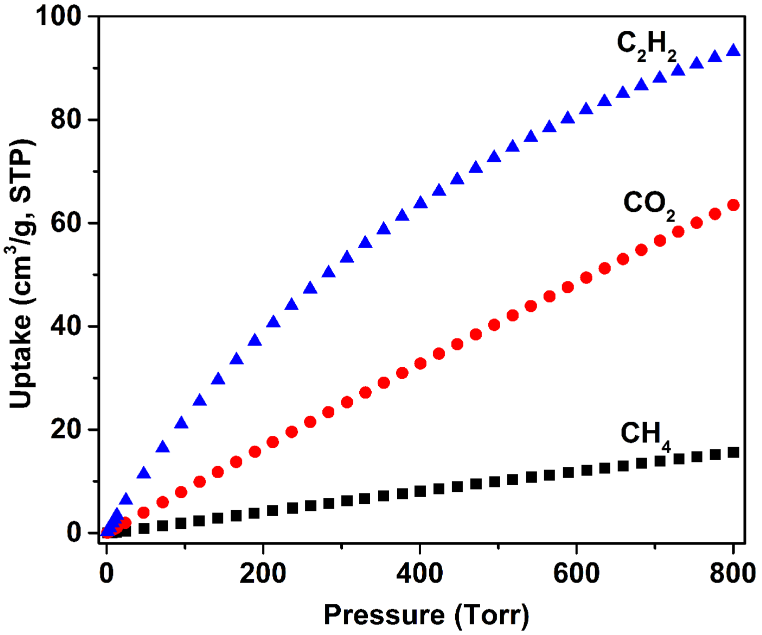

Figure S9. Gas sorption isotherms of **1a** for C_2H_2, CO_2 and CH_4 at 273K.

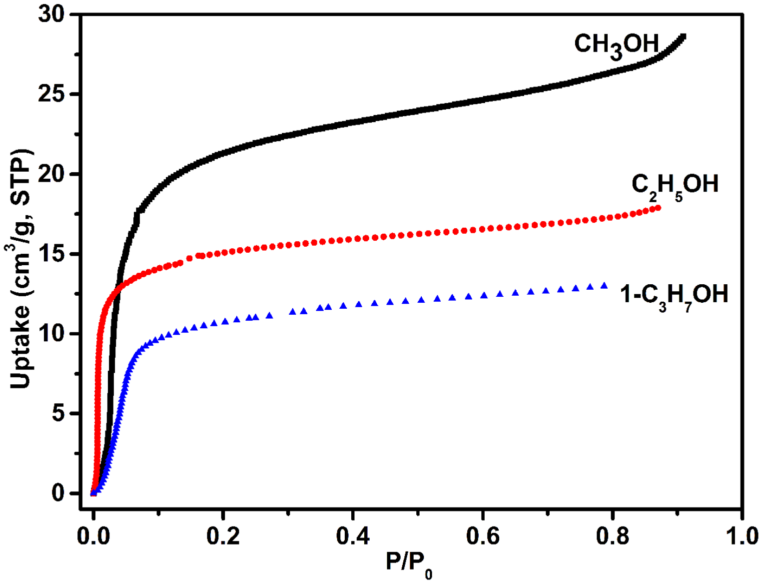

Figure S10. Vapor sorption isotherms of **1a** for methanol, ethanol and propanol at room temperature.

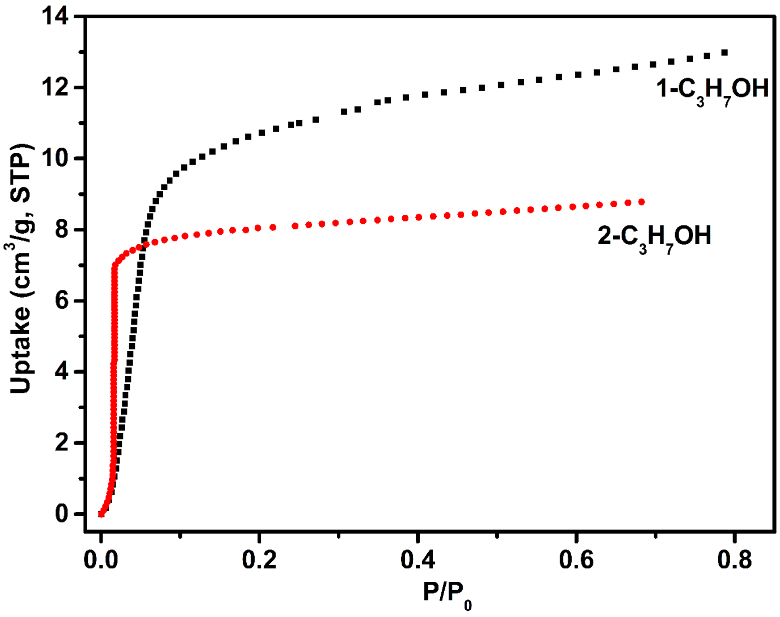

Figure S11. Vapor sorption isotherms of **1a** for propanol and isopropanol at room temperature.

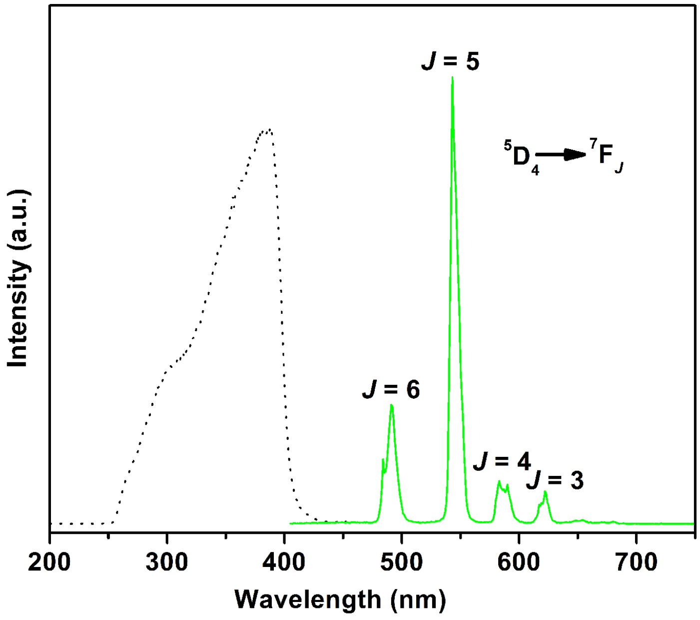

Figure S12. The excitation and PL spectrum of solid **1a** (monitored and excited at 544 and 382 nm, respectively).

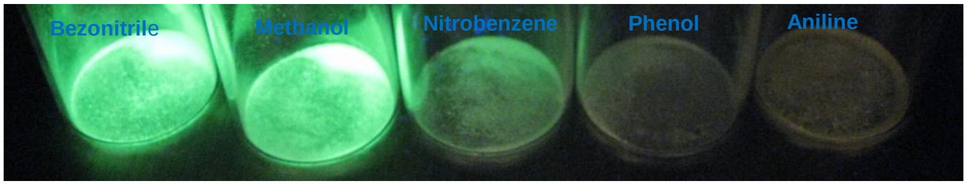

Figure S13. The photo images of **1a** in the presence of various guest molecules (excited at 365 nm).

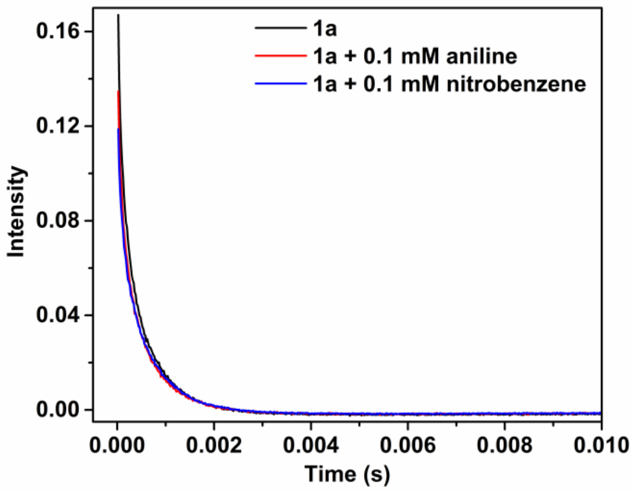

Figure S14. Fluorescence decay data of **1a** in methanol (0.5 mg/ml) monitored at 545 nm at room temperature (excited at 304 nm). The decay curves are well fitted with a double exponential function and yield a lifetime of 0.52 ms for the three samples.

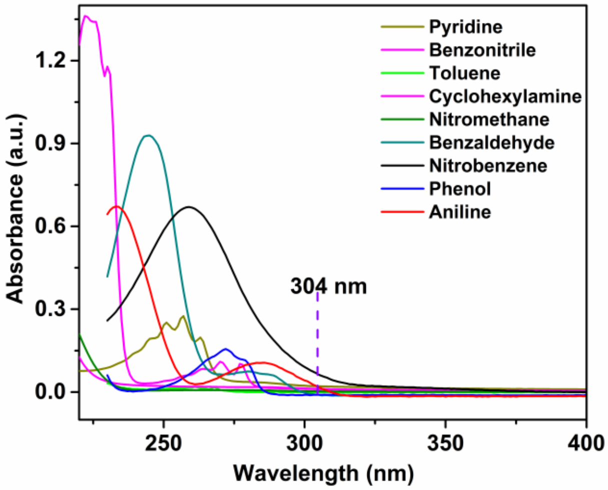

Figure S15. The UV-vis absorption spectra of guest molecules in methanol (0.1 mM).

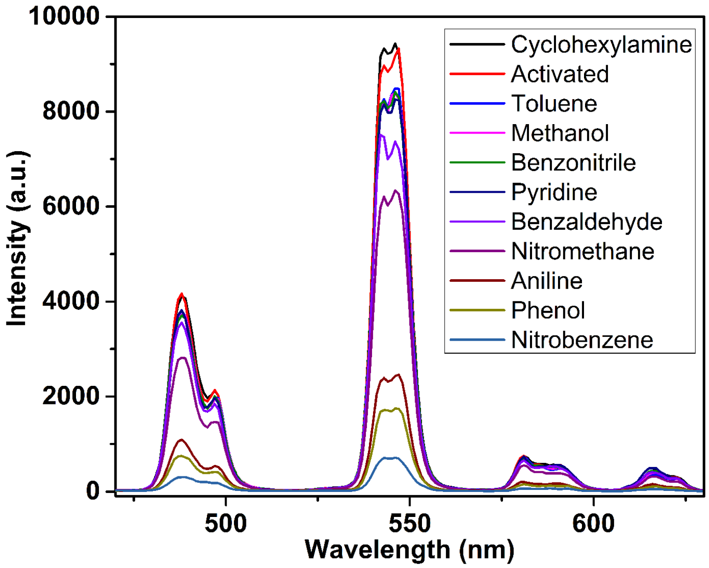

Figure S16. The PL spectra of MOF-76a introduced into various guest molecules when excited at 304 nm.

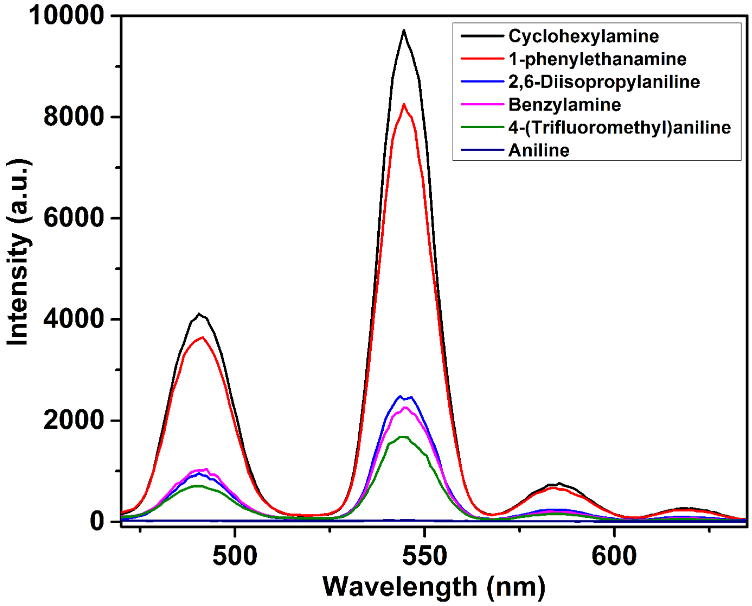

Figure S17. The PL spectra of **1a** introduced into various amine molecules when excited at 304 nm.

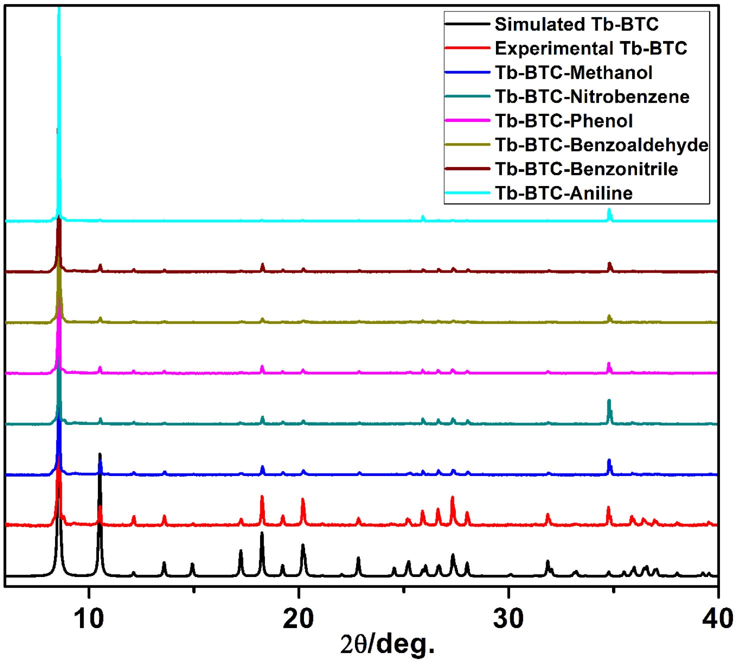

Figure S18. PXRD patterns of Tb-BTC.

1. Derivation of the Isosteric Heats of Adsorption: A virial-type expression of comprising the temperature-independent parameters a_i and b_j was employed to calculate the enthalpies of adsorption for CO_2, CH_4 and C_2H_2 (at 273 K and 296 K).[1-2] In each case, the data were fitted use equation:

$$\ln P = \ln N + 1/T \sum_{i=0}^{m} a_i N^i + \sum_{j=0}^{n} b_j N^j \quad (1)$$

Here, P is the pressure expressed in Pa, N is the amount absorbed in mmol g^{-1}, T is the temperature in K, a_i and b_j are virial coefficients, and m, n represent the number of coefficients required to adequately describe the isotherms (m and n were gradually increased till the contribution of extra added a and b coefficients was deemed to be statistically insignificant towards the overall fit. And the average value of the squared deviations from the experimental values was minimized). The values of the virial coefficients a_0 through a_m were then used to calculate the isosteric heat of absorption using the following expression:

$$Q_{st} = -R \sum_{i=0}^{m} a_i N^i \quad (2)$$

Q_{st} is the coverage-dependent isosteric heat of adsorption and R is the universal gas constant of 8.3147 J $K^{-1}mol^{-1}$. The heat enthalpy of CO_2, CH_4 and C_2H_2 sorption for complex **1a** in this manuscript are determined by using the sorption data measured in the pressure range from 0-1 bar (273 K).

2. Dual Site Langmuir-Freundlich Model for C_2H_2/CH_4, and CO_2/CH_4 Adsorption Isotherms

On the basis of the Dual site Langmuir-Freundlich (DSLF) model: (**I**)

$$N = N_1^{\max} \times \frac{b_1 p^{1/n1}}{1+b_1 p^{1/n1}} + N_2^{\max} \times \frac{b_2 p^{1/n2}}{1+b_2 p^{1/n2}} \quad \textbf{(I)}$$

where p (unit: kPa) is the pressure of the bulk gas at equilibrium with the adsorbed phase, N (unit: mol/Kg) is the adsorbed amount per mass of adsorbent, $N1^{max}$ and $N2^{max}$ (unit: mol/Kg) are the saturation capacities of sites 1 and 2, b1 and b2 (unit: 1/kPa) are the affinity coefficients of sites 1 and 2, and n_1 and n_2 represent the deviations from an ideal homogeneous surface. Here, the single-component C_2H_2, CO_2, and CH_4, adsorption isotherms have been fit to enable the application of IAST in simulating the performance of **1a** under a mixed component gas. The fitting parameters of DSLF equation are listed in Table S2. Adsorption isotherms and gas selectivities calculated by IAST for mixed C_2H_2/CH_4 (C_2H_2/CH_4 = 50:50 and CO_2/CH_4 (CO_2/CH_4 = 50:50) in the **1a**.

In order to confirm the excellent gas selectivities in **1a**, the well-known ideal adsorbed solution theory (IAST) calculation is also applied to estimate the C_2H_2/CH_4 and CO_2/CH_4 adsorption selectivity. Mixture adsorption isotherms and the selectivities at different pressures and temperatures calculated by IAST for mixed C_2H_2/CH_4 (C_2H_2/CH_4 = 50:50) and CO_2/CH_4 (CO_2/CH_4 = 50:50) in this activated MOF as a function of total bulk pressure are shown in Figures S17 and S18.

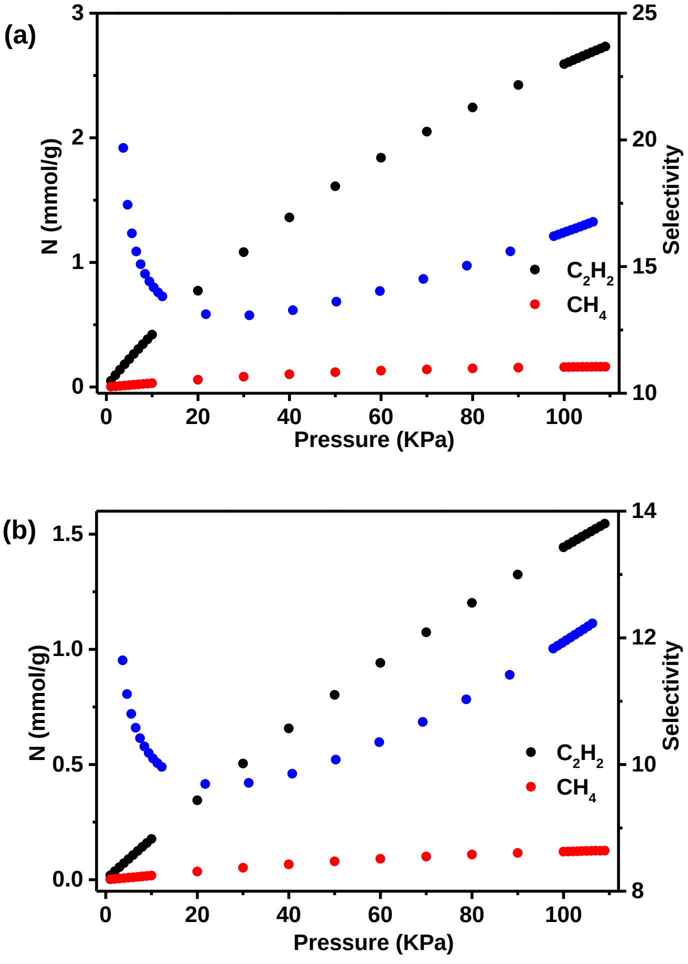

Figure S19. Mixture adsorption isotherms and adsorption selectivity predicted by IAST of **1a** for C_2H_2 (50%) and CH_4 (50%) (a, b) at 273 and 296 K, respectively.

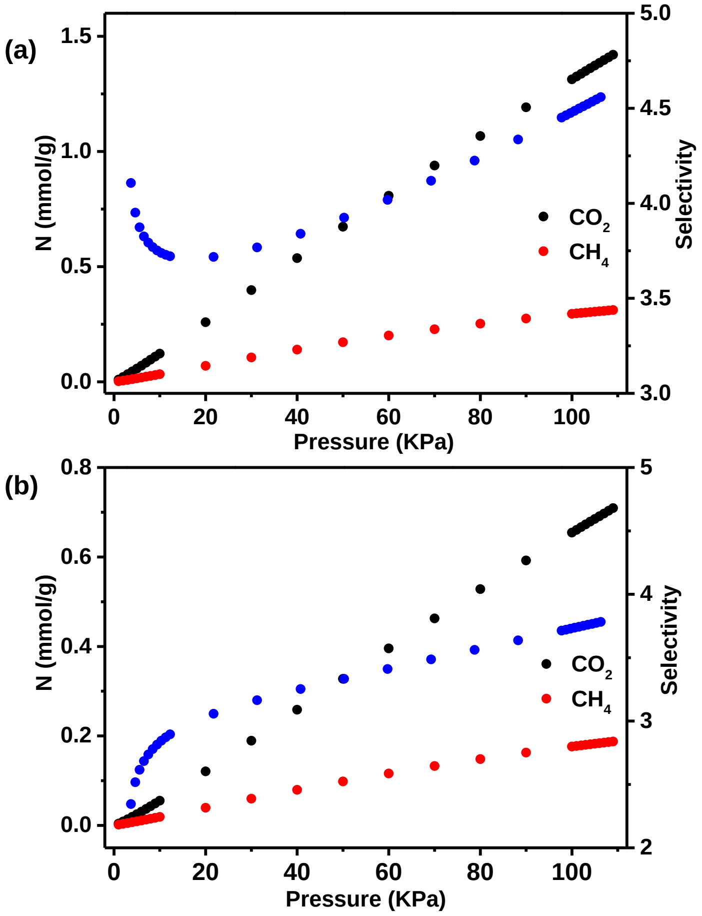

Figure S20. Mixture adsorption isotherms and adsorption selectivity predicted by IAST of **1a** for CO_2 (50%) and CH_4 (50%) (a, b) at 273 and 296 K, respectively.

Table S1. IAST selectivities of C_2H_2/CH_4 (C_2H_2/CH_4 = 50:50) and CO_2/CH_4 (CO_2/CH_4 = 50:50).

mixture	Temperature (K)	component proportion	IAST selectivity
C_2H_2/CH_4	273	50:50	19.7
CO_2/CH_4	273	50:50	4.1
C_2H_2/CH_4	296	50:50	11.6
CO_2/CH_4	296	50:50	2.3

Table S2. Equation parameters for the DSLF isotherm model.

Adsorbates	N_1^{max} (mmol/g)	b_1 (kPa^{-1})	$1/n_1$	N_2^{max} (mmol/g)	b_2 (kPa^{-1})	$1/n_2$
C_2H_2 (273 K)	4.65613	0.01209	0.8844	3.88253	0.01027	1.02802
CH_4 (273 K)	0.36601	0.0011	1.20105	2.14687	0.00188	1.14364
CO_2 (273 K)	5.00076	0.00239	1.00829	6.15277	0.00139	1.20964
C_2H_2 (296 K)	4.50236	0.00463	0.93084	4.59139	0.00337	1.06875
CH_4 (296 K)	0.93284	0.00073305	1.29051	0.76385	0.00312	0.96429
CO_2 (296 K)	3.29116	0.0014	1.20895	2.04234	0.00193	1.07632

---

1 J. Roswell, O. M.Yaghi, *J. Am. Chem. Soc.*, 2006, **128**, 1304.

2 R. Banerjee, H. Furukawa, D. Britt, C. Knobler, M. O'Keeffe and O. M. Yaghi, *J. Am. Chem. Soc.*, 2009, **131**, 3875.